ASTRALUX INC.
FINAL REPORT: 1/21/97 - 1/21/98
ADVANCED UV DETECTORS AND DETECTOR ARRAYS
CONTRACT NO. NASW-97006

1. INTRODUCTION:

Gallium Nitride (GaN) with its wide energy bandgap of 3.4 eV holds excellent promise for solar blind UV detectors. We have successfully designed, fabricated and tested GaN p-i-n detectors and detector arrays. The detectors have a peak responsivity of 0.14A/W at 363 nm (3.42 eV) at room temperature. This corresponds to an internal quantum efficiency of 56%. The responsivity decreases by several orders of magnitude to 0.008 A/W at 400 nm (3.10 eV) giving the excellent visible rejection ratio needed for solar-blind applications.

2. EXPERIMENT:

Device design:

We chose the standard mesa structure design for the GaN p-i-n detectors to allow for efficient detection of light incident normal to the surface. A schematic of the device design is shown in Fig.1.

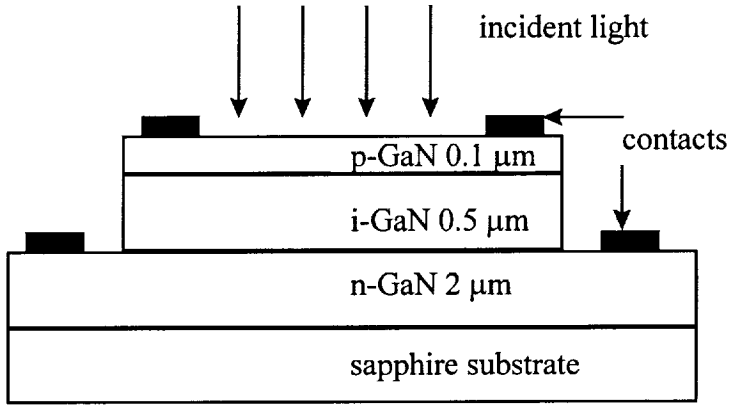

Fig.1. Cross section of GaN p-i-n detector structure.

The reason for using a p-i-n type detector is to optimize the internal quantum efficiency by absorbing the light (which generates e-h pairs) in the thick photosensitive i-layer. The e-h pairs are separated by the internal electric field (in photovoltaic mode) or by a stronger electric field when under reverse bias (photodiode). The top p-layer must be thin to transmit light to the photosensitive i-layer. However, if the p-layer is too thin, the series resistance will increase and the device speed will suffer. The doping should be high for contact purposes, but not too high because high doping tends to degrade the material quality. We chose a p-layer thickness of 0.1 μm and a doping of $\sim 10^{18}$ cm^{-3} to optimize the trade-off between series resistance and optical absorption. The undoped photosensitive i-layer was chosen at 0.5 μm, allowing for sufficient absorption of the

incident light. The n-layer is 2-μm-thick (not critical) with a carrier concentration of 10^{18} cm^{-3} for contact purposes.

Due to unforeseen delays in upgrading our MOCVD reactor to RF-heating, the GaN wafer used in these experiments was purchased from SVT Associates, Inc.[1] A new 5kW RF-generator is now in place and the custom SiC-coated graphite susceptors ordered from SGL Carbon Group [2] are scheduled to be shipped ~1/28/98. We should therefore be able to grow the layers "in house" soon thereafter.

Mask design:

We designed and fabricated a mask for GaN p-i-n detectors and detector arrays. The active areas of the detectors range from 125x125 μm^2 to 325x325 μm^2. A typical optical image of the completed detectors are shown in Fig. 2.

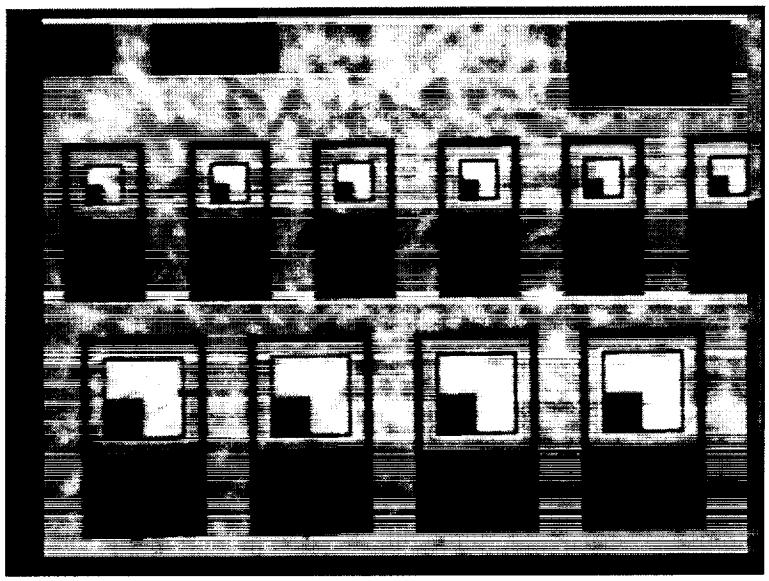

Fig. 2. GaN p-i-n detectors of sizes; 125x125 μm^2 and 225x225 μm^2. The image is taken while illuminated by light in transmission which is why the contacts appear black. The gray areas are the etched GaN, and the light areas are the unetched mesas.

Rectangular and cross-hair-type p-contacts (see Fig. 3) with bonding pads are used to allow sufficient open areas for the incident light to penetrate into the detector. There are 15 - 30 detectors in each array depending on individual device size. A part of two detector arrays with the cross-hair-type contacts are shown in Fig. 3.

[1] SVT Associates, Inc., Eden Prairie, MN 55344
[2] SGL Carbon Group, Dallas, TX 75247

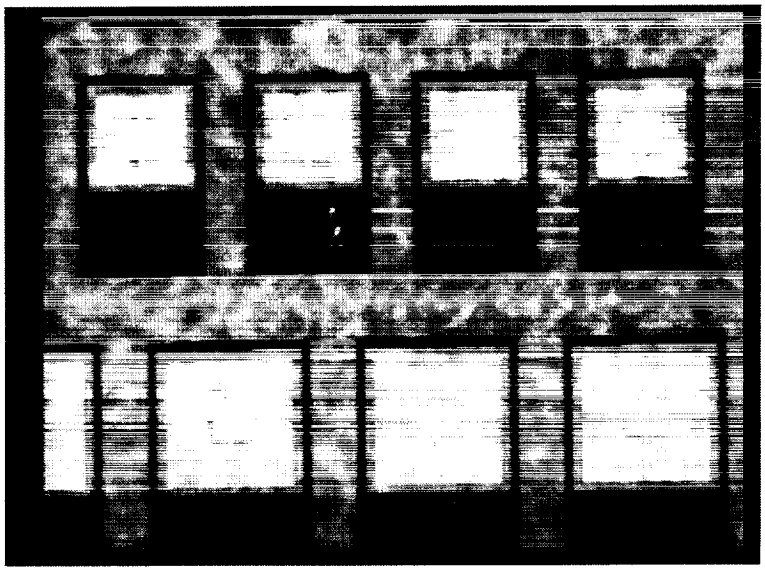

Fig. 3. GaN p-i-n detectors with cross-hair-type p-contacts. This picture is taken under front illumination. The p-GaN contacts are the white cross hairs on the square mesas. The black areas are the n-GaN contacts, and the gray areas are the etched GaN. The detector sizes are 125x125 μm^2 and 225x225 μm^2.

Device fabrication:

The detector fabrication consists of three process steps: 1) mesa etch (device isolation), 2) p-contacts, and 3) n-contacts. Unfortunately, GaN is very inert so chemical wet etching has proven difficult at reasonable temperatures. The mesa etch is therefore performed using reactive ion etching (RIE) with a CCl_2F_2 (Freon 12) gas. A typical etch is performed at a power density of ~0.5 W/cm^2 and at a pressure of 50 mTorr yielding an etch rate of ~ 60 nm/min. We used patterned photoresist as the etch mask. A trace over two adjacent detectors using a surface profilometer is shown in Fig. 4.

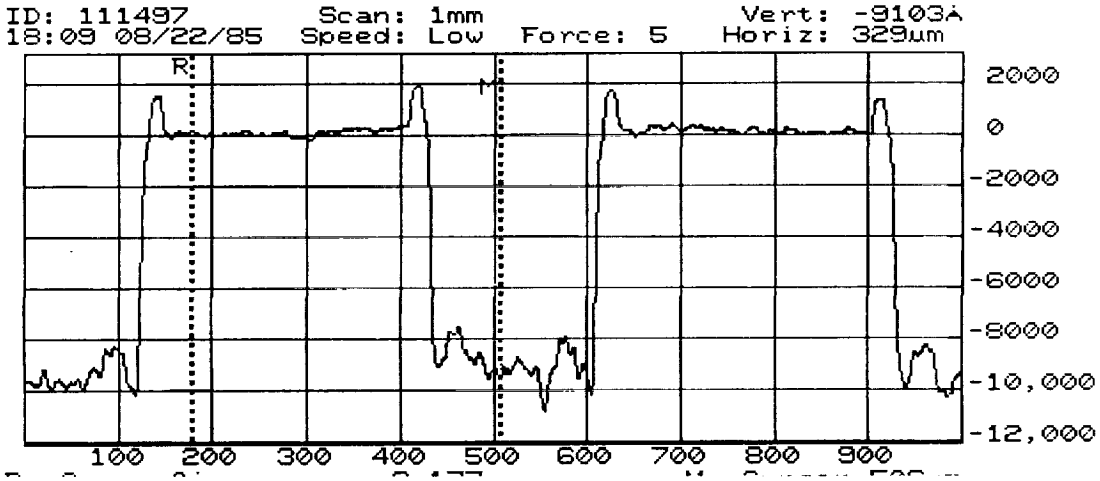

Fig. 4. Surface profile of the two adjacent detectors in an array. The scales on the x- and y-axis are µm and Å, respectively. Each detector is 325 µm wide.

The "spikes" on the edges of the detector mesas are the ~ 180 nm-thick p-contacts as seen in Fig. 1. The etch depth is ~ 1 μm, and the increased surface roughness in the etched trenches is clearly visible. The rough surface resulting from the RIE treatment can also be seen in Figs. 3 where the n-contact metal appears black due to light scattering. For comparison, the p-contacts on the unetched mesa reflect the light brilliantly. Photoresist is not a good RIE mask because it etches relatively fast (R ~ 110 nm/min under above-mentioned conditions). Dielectrics such as SiO_2 or Si_3N_4 are better masking materials due to higher etch resistance, and they are less prone to cracking or flaking due to heating in the chamber. Dielectric masks therefore allow for etching at higher powers to obtain vertical sidewalls. We will use PECVD oxides in the next set of devices.

The n- and p-contacts are Ti/Ni/Au and Ni/Au, respectively. The metal layers were deposited using an e-beam evaporator at pressures lower than 10^{-6} Torr. The contacts were formed using the photoresist lift-off technique. In this first batch of devices the contacts were not annealed. A high temperature anneal (typically >800°C for n-contact and >500°C for p-contact) can improve the contact resistance for both n and p-type contacts.[3] However, when measuring the detector response in the photovoltaic mode the photocurrent is relatively low, and thus, the IR-drop across the contacts is small. The RC time constant is increased due to large contacts resistance. Therefore we will anneal the next batch, which should allow for high speed operation.

Testing:

a) Electrical testing:

The current-voltage (I-V) characteristics of the detectors were measured using an HP 4145B semiconductor parameter analyzer and probe station. Typical traces are shown in Fig. 5.

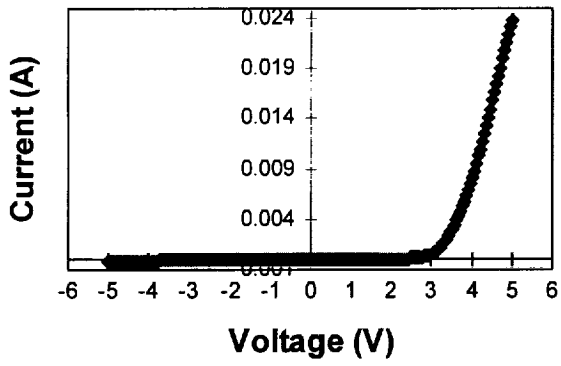

Fig. 5. I-V characteristics from a 225x225 μm^2 GaN p-i-n UV detector.

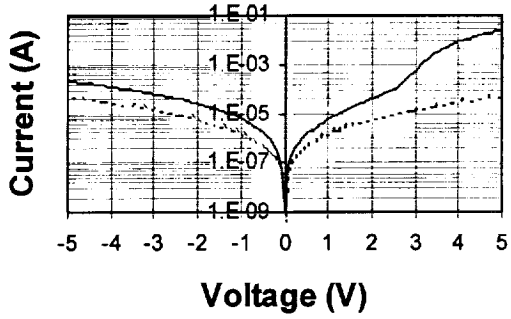

Fig. 6. I-V characteristics from a 225x225 μm^2 GaN p-i-n UV detector.

[3] J.M. Van Hove et al. *Appl. Phys. Lett.* **70** (17) p. 2282, (1997).

On the linear scale the rectification under forward bias and the little leakage current under reverse bias give the appearance of an ideal diode. Unfortunately, if we look at the trace on a semilog plot is becomes apparent that there is a large leakage current in these devices. We attribute the leakage current to surface damage along the diode mesa edges caused by RIE. We confirmed this by probing two adjacent diodes, which in principle should be isolated. The symmetric reverse leakage current from these back-to-back diodes is shown by the broken line in Fig. 6. The onset of the desired injection current at roughly 2.5 V is clearly seen under forward bias in Fig 6. This is roughly the expected "onset" voltage of a wide bandgap semiconductor with bandgap of 3.4 eV.

We intend to pursue three alternatives to reduce the unwanted leakage current in these detectors: 1) Improve the RIE process by using dielectric masks, 2) Passivate the junctions using PECVD oxide, and 3) selectively grow the mesa structures using MOCVD (See section on future work).

The capacitance-voltage (C-V) characteristics of these detectors were measured using a HP LCR meter (in parallel mode). A typical $1/C^2$-V trace is shown in Fig. 7.

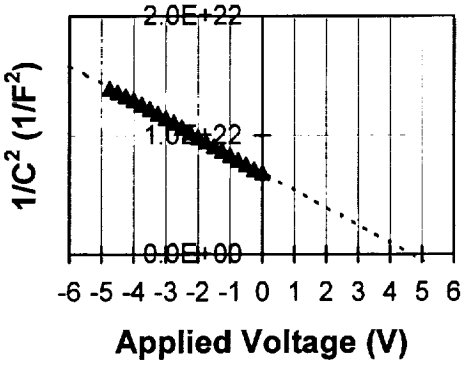

Fig. 7. $1/C^2$-V plot from a 225x225 μm^2 GaN p-i-n detector.

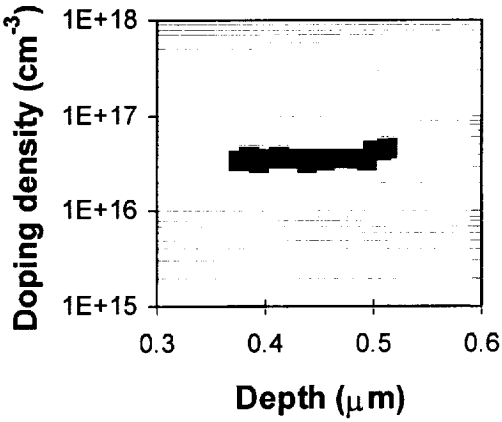

Fig. 8. Doping density in the "intrinsic" layer.

The built-in potential (x-axis intercept) and the doping density (slope) can be extracted from the $1/C^2$-V trace. The contacts were not annealed yet, so there is some constant series capacitance shifting the curve (Fig. 7) up making it difficult to estimate the built-in potential. However, since the doping density in the i-layer is orders of magnitude less than in both the n-and p-layers, the reverse bias only depletes the i-layer, and thus the doping density in the i-layer can be estimated as shown in Fig. 8. Also note that at 0.5 μm the doping density increases confirming the thickness of the i-layer. We will monitor the C-V characteristics of the detectors as the contacts are annealed and the junctions are passivated.

b) Optical testing:

Since the reverse leakage current was relatively high in these detectors, we measured the responsivity in the photovoltaic mode (no applied bias). We used a

tungsten lamp dispersed through a prism spectrometer as the light source. The devices were probed directly, and the generated photovoltage was detected using a lock-in amplifier. The signal was converted to an absolute scale (A/W) using a calibrated UV-enhanced Si detector. The responsivity as a function of wavelength is shown in Fig. 9.

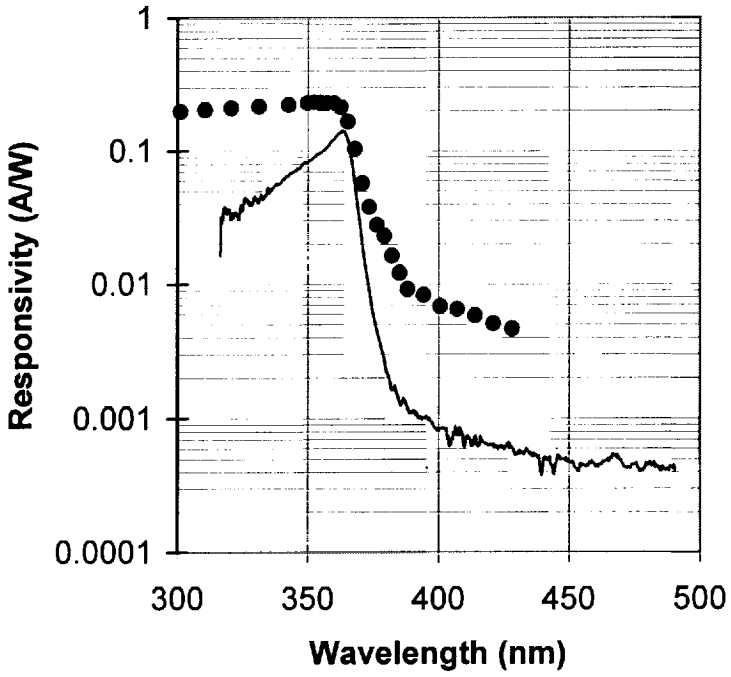

Fig. 9. Responsivity of 225x225 μm^2 GaN p-i-n detector (solid line). The quantum efficiency limit (η_{int}= 1) is plotted (black circles) for comparison.

The responsivity of a p-i-n diode can be estimated using Eqs. 1 and 2 and is plotted in Fig. 9 using black circles:

$$R = \eta_{\text{int}} \frac{q}{h\nu}\left(1 - e^{-\alpha L}\right)(1 - r) \tag{1}$$

$$r = \left(\frac{n_{GaN} - n_{air}}{n_{GaN} + n_{air}}\right)^2 \tag{2}$$

The absorption coefficient and the refractive index data were taken from the literature.[4,5]

The measured peak responsivity is 0.14 A/W at 363 nm (3.42 eV), which is consistent with results published by other groups.[6,7] The visible rejection ratio is

[4] J.I. Pankove et al. *Appl. Phys. Lett,* **17** (5), p. 197 (1970).
[5] I. Akasaki, et al. *Mat. Res. Soc. Symp. Proc.,* **339**, p. 443 (1994).
[6] J.M. Van Hove et al. *Appl. Phys. Lett.* **70** (17) p. 2282, (1997).
[7] G.Y. Xu et al. *Appl Phys. Lett.* **71** (15) p. 2154, (1997).

several orders of magnitude from 363 nm to 400 nm, at which we have reached the noise level. The signal level is simply limited by a weak UV light source which is further attenuated by passing the light through 0.5 mm slits in the spectrometer. The true visible rejection ratio is probably larger, and will be measured in the near future by the use of a deuterium source.

3. FUTURE WORK:

During the first year, we have demonstrated our capabilities in manufacturing GaN-based UV detectors and detector arrays. This effort has included materials growth, device design, processing technology and device characterization. More specifically, we have:

- Grown high quality GaN films with electron mobility higher than 350 cm^2/V-sec.
- Grown Mg-doped GaN either p-type or exhibiting high photoconductivity to dark conductivity ratio.
- Optimized the growth conditions through measurements of $\eta\mu\tau$ product of undoped and Mg-doped GaN films.
- Fabricated prototype p-i-n UV detectors and detector arrays using RIE.
- Studied responsivity of the prototype detectors.

With these key technologies in place, we are confident that we are able to develop and deliver state-of-art UV detectors and detector arrays. The first year's effort has paved the way for further optimization of the detectors in the second year. In particular, we will:

- Fabricate a n-i-p structure using n-type AlGaN as the window layer and a p-type GaN as the bottom layer. The benefit of using the n-type layer as the window layer is because the $\eta\mu\tau$ product of n-type films is much higher than the $\eta\mu\tau$ product of the p-type layer. In fact, photons absorbed in the p-type GaN layer contribute very little to the detector response because the $\eta\mu\tau$ product is several orders of magnitude lower in p-type films.
- Reduce the thickness of the window layer to 50 nm or less.
- Reduce the thickness of the i-layer to about 100 nm. This thickness is enough to absorb all light with photon energies higher than 3.2 eV. Such a detector with a thin i-layer will absorb few photons in the visible and near UV and thus enable an even sharper cut-off near the band gap of GaN. We shall continue the optimization of the i-layer by reducing the defect density to improve further the responsivity.
- Optimize the processing technology to reduce process-induced damage and the leakage current.

Additional experiments that will be performed on the first generation detectors:

- Measure the true visible rejection ratio.
- Anneal contacts and passivate junctions with SiO_2.

When the leakage current is reduced and contacts annealed we will:

- Measure time decay (response time).
- Perform noise measurements.

In addition to the tasks outlined above we will try a novel approach to selectively grow the p-i-n junctions. This can be done using patterned SiO_2 on GaN/sapphire substrates with MOCVD. We have already grown n-GaN mesas using MOCVD as shown in Fig. 10. Note that it is difficult to selectively grow GaN using MBE with elemental sources.[8]

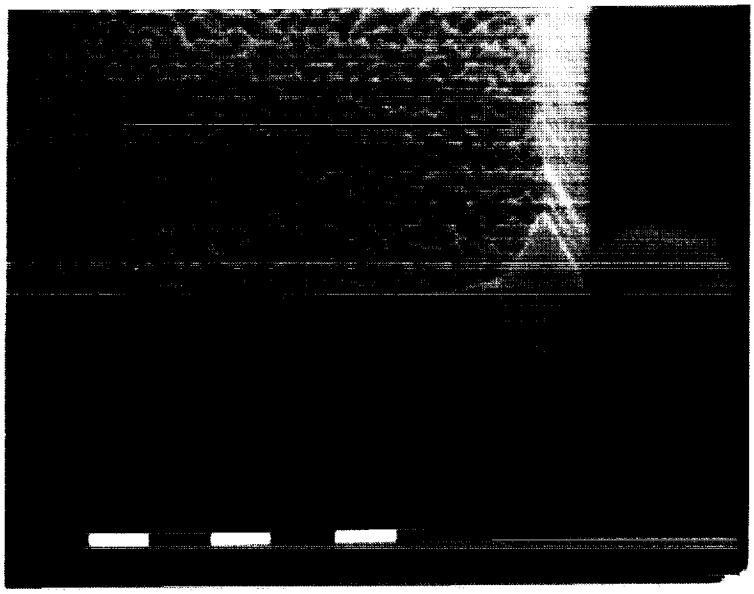

Fig. 10. Selectively grown GaN in SiO_2 windows. The markers are 1 μm.

Using selective growth, the RIE step is eliminated and leakage current should be significantly reduced. To the best of our knowledge, most GaN diodes devices published to date suffer from poor reverse bias characteristics. This includes the super-bright blue and green Nichia LEDs. This is especially true for p-i-n detectors with heavily doped p-contact layers. This leakage probably comes form the RIE processing step and reduced p-layer quality.

4. CONCLUSION:

GaN p-i-n detectors and detector arrays have been fabricated and tested The detectors have a peak responsitity of 0.14A/W at 363 nm (3.42 eV). This corresponds to an internal quantum efficiency of 56%. The responsivity decreases by several orders of magnitude to 0.008 A/W at 400 nm (3.10 eV) giving the excellent visible rejection ratio needed for solar blind applications.

[8] J.T. Torvik et al. *Appl. Phys. Lett,* **72**, 244 (1998).

REPORT DOCUMENTATION PAGE

Form Approved
OMB No. 0704-0188

1. AGENCY USE ONLY *(Leave blank)*	2. REPORT DATE	3. REPORT TYPE AND DATES COVERED
	26 JAN 98	Final Report 21JAN 97 - 21JAN 98

4. TITLE AND SUBTITLE
Advanced UV Detector and Detector Array

5. FUNDING NUMBERS
NASW-97006

6. AUTHOR(S)
Jacques I. Pankove and John Torvik

7. PERFORMING ORGANIZATION NAME(S) AND ADDRESS(ES)
Astralux, Inc.
2500 Central Avenue
Boulder, CO 80301-2845

8. PERFORMING ORGANIZATION REPORT NUMBER
7200

9. SPONSORING/MONITORING AGENCY NAME(S) AND ADDRESS(ES)
National Aeronautics & Space Administration
Headquarters Acquisition Division, Code CW
Washington, D.C. 20546

10. SPONSORING/MONITORING AGENCY REPORT NUMBER

11. SUPPLEMENTARY NOTES

12a. DISTRIBUTION/AVAILABILITY STATEMENT
Distribution authorized to U.S. government agencies only. Other requests shall be referred to the performing organization in Block 7 of this form.

12b. DISTRIBUTION CODE

13. ABSTRACT *(Maximum 200 words)*

During the first year of this project, Astralux has demonstrated the capability of growing high quality GaN films and fabricating prototype p-i-n UV detectors. These detectors have a responsivity of 0.14 A/W at 363 nm and more than two orders of magnitude drop in sensitivity to visible light. This performance is comparable to that reported by other researchers. However these detectors were not passivated. Hence a substantially better response is expected from detectors that will be fabricated in the second year.

14. SUBJECT TERMS
UV detector III-Nitrides GaN
Photoconductivity Deposition system

15. NUMBER OF PAGES
8

16. PRICE CODE

17. SECURITY CLASSIFICATION OF REPORT	18. SECURITY CLASSIFICATION OF THIS PAGE	19. SECURITY CLASSIFICATION OF ABSTRACT	20. LIMITATION OF ABSTRACT
unclassified	unclassified	unclassified	SAR

NSN 7540-01-280-5500

Standard Form 298 (Rev. 2-89)
Prescribed by ANSI Std. 239-18
298-102